

Check for updates

# Nanosecond Laser Debonding Using an Ultrathin Absorber Layer in a Transparent Composite: Making a Light-Powered Exploding Bolt

Touhid Bin Anwar and Christopher J. Bardeen\*

Localized heating of an adhesive interface can separate glued substrates for recycling or reconfiguring. Light provides a way to deposit energy at this type of buried interface, but the photon energy must still be transformed into thermal energy. The deposition of an ultrathin (<1 µm) absorbing layer before gluing provides a way to build this photothermal capability into the bonded structure. To demonstrate this concept, a submicron absorbing layer composed of the dye Fluorescein 27 (F27) is applied to a poly(methyl methacrylate) (PMMA) substrate that is glued to a second PMMA piece using a commercial cyanoacrylate adhesive. The laser debonding is characterized as function of dye layer thickness, applied pressure, and laser pulse fluence. A 450 nm thick dye layer retained a high adhesive strength of 3.5 MPa but can be debonded by a single 532 nm nanosecond laser pulse with a fluence ≤ 0.7 J cm<sup>-2</sup>. Decomposition of the absorbing layer resulted in rapid gas evolution that left the micron-scale surface morphology of the PMMA substrate intact. This system enabled the fabrication of an optical analog to the exploding bolt, where a single laser pulse can impulsively separate a structural fastener.

# 1. Introduction

The use of chemical adhesives is rapidly expanding due to their low cost and light weight.<sup>[1]</sup> An increasing number of everyday objects rely on chemical adhesives to create durable, lightweight, composite structures, from laminated solar panels to phone displays to automobile bodies. But the same adhesive properties that make these objects so durable also make them challenging to disassemble.<sup>[2]</sup> Separation of glued substrates is often required for recycling objects that have reached the end of their useful lives.<sup>[3]</sup> Alternatively, it may be desirable to reconfigure some

T. B. Anwar Department of Chemical Engineering University of California Riverside Riverside, CA 92521, USA

C. J. Bardeen
Department of Chemistry
University of California Riverside
Riverside, CA 92521, USA
E-mail: christopher.bardeen@ucr.edu

The ORCID identification number(s) for the author(s) of this article can be found under https://doi.org/10.1002/adfm.202410080

DOI: 10.1002/adfm.202410080

parts of a glued object, which also necessitates rupturing the adhesive bonds. A dramatic example of this type of mechanical reconfiguring would be an exploding bolt that jettisons part of a spacecraft after launch.<sup>[4]</sup>

The challenge of debonding two objects has been addressed from several different angles. For weak adhesives, the application of physical pressure can be sufficient to separate the bonded objects, although this force can also damage the objects themselves. For stronger adhesives, the bonded area can be exposed to heat or solvent in order to melt or dissolve the adhesive.[5] This process is typically slow and requires the bonded substrates to be exposed to the same harsh conditions that degrade the glue. Custom adhesives that contain photochemically active molecules can respond to an external light source by undergoing liquefication or polarity changes that result in loss of adhesion.<sup>[6]</sup> Light-sensitive glues show promise, but it is not clear

that their bonding mechanisms can match the performance of standard adhesives like epoxies and cyanoacrylates. Our group recently developed a light-based debonding strategy in which a nanosecond laser pulse generates impulsive heating at the adhesive-substrate interface. [7] Poly(methyl methacrylate) (PMMA) was attached to aluminum (Al) using cyanoacrylate (CA) adhesive, commonly known as "super glue", to demonstrate that a single nanosecond laser pulse could destroy the strong CA-Al adhesive bond and separate the objects. The pulse energy was absorbed primarily at the Al surface, which led to localized heating that disrupted both mechanical (due to surface roughness) and chemical adhesion. Subsequent diffusion of the heat produced by the single laser pulse resulted in a negligible temperature rise across the larger assembly. Furthermore, the separation left a minimal amount of residue on the Al surface and did not require the use of organic solvents. We hypothesized that impulsive laser heating of the adhesive interface could provide a general strategy to debond objects without the need to develop new stimuli-responsive glues.

The CA-Al nanosecond laser debonding relied on the fact that one of the bonded surfaces was a metal that could readily absorb a large fraction of the incoming light and rapidly heat up. If neither substrate absorbs at the laser wavelength, then the deposition of heat at the interface becomes a challenge. Our solution

www.afm-journal.de

1616938.0, Downloaded from https://onlinelibtrary.wiley.com/doi/10.1002/afm.2024.10080 by Christopher Bardeen - University Of California, Wiley Online Library on [21/08/2024], See the Terms and Conditions (https://onlinelibtrary.wiley.com/terms-and-conditions) on Wiley Online Library for rules of use; OA articles are governed by the applicable Cerative Commons

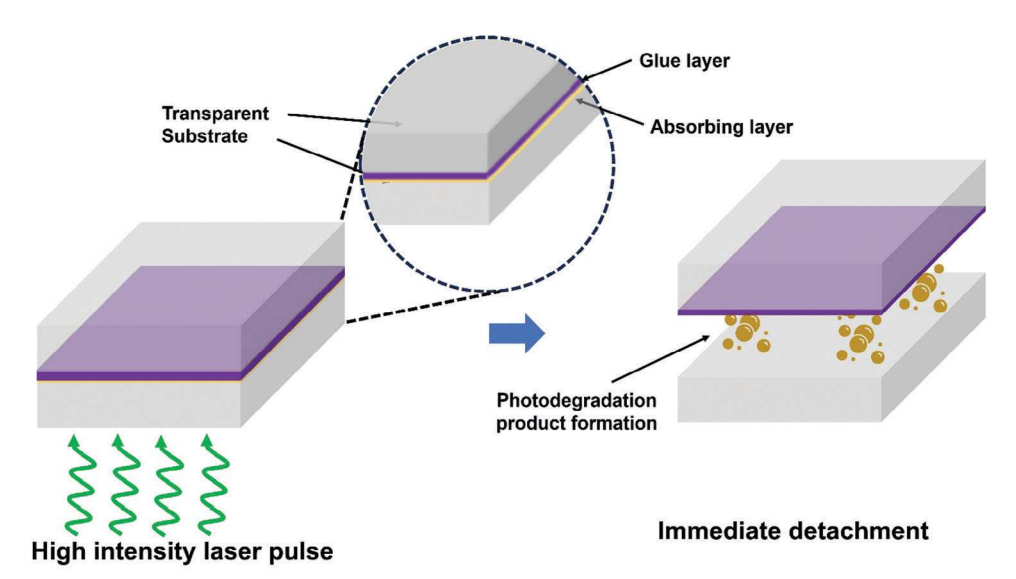


Figure 1. Schematic illustration of how an ultrathin absorber layer sandwiched between transparent substrates can enable impulsive laser heating at the interface and debonding.

is to insert a highly absorbing layer between the two transparent substrates that can generate impulsive heating at the interface. In practice, such a layer would be applied to the substrate before gluing as an absorber layer that resides at the interface between the adhesive and the substrate, as outlined in **Figure 1**. This absorber layer must fulfill several requirements. First, it must be ultrathin so that it does not interfere with the mechanical adhesion, allowing it to maintain close to the original adhesive strength. Second, it must provide high absorption at the laser wavelength, and efficiently convert the incident photon energy to heat. If successful, this strategy should make it possible to generalize the laser debonding method across a larger class of materials that are transparent at the debonding laser wavelength.

In this work, we show that submicron films composed of the dye Fluorescein 27 (F27) can fulfill this role. In aggregated form, this dye can provide a homogeneous coating that provides high absorption accompanied by rapid heat generation. To demonstrate the concept in Figure 1, a commercial CA was used to glue a transparent PMMA substrate to a second PMMA piece with an ultrathin dye layer. Debonding of this composite structure by 532 nm laser pulses was characterized as function of film thickness, applied pressure, and laser pulse fluence. In addition to surface melting, the mechanism of debonding appears to involve the decomposition of the F27 layer accompanied by explosive gas evolution. The micron-scale morphology of the PMMA substrate was not significantly changed by the impulsive debonding process, demonstrating that this method causes minimal damage to the bonded surfaces. The ability to initiate a single-shot debonding of two PMMA pieces allowed us to create transparent plastic bolts that can be severed using light. Our results show that the nanosecond laser pulse debonding method has the potential to be applied to any substrate where an ultrathin absorbing layer can be applied, without requiring that one of the substrates absorb the laser light itself.

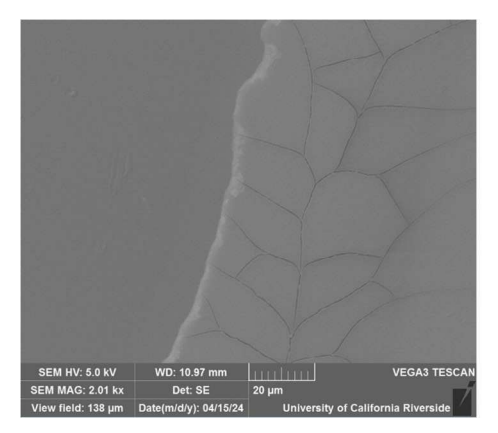
## 2. Results and Discussion

To apply the absorbing layer, we had to take PMMA's vulnerability to hydrophobic solvents into account. To prevent dissolution and cracking of the PMMA surface, [8] we used a hydrophilic solvent system (ethanol/water) to apply the absorber layer. We first attempted to spin-coat aqueous suspensions of traditional photothermal absorbers like carbon nanotubes and gold nanoparticles but found these particles aggregated during the coating process, leading to spatially heterogeneous films that did not support strong adhesion or effective debonding (Figure S2, Supporting Information). Ionic dyes like Rose Bengal, Malachite Green, and F27, on the other hand, provided much more homogeneous coatings when deposited from ethanol-water mixtures (Figure S3, Supporting Information). The xanthene dyes have the additional advantage of extremely large absorption coefficients, on the order of  $10^5$  m<sup>-1</sup>cm<sup>-1</sup>, near the 532 nm output wavelength of our nanosecond pulsed laser. Finally, xanthene dyes have high thermal stability [9] and high photostability under low light conditions, [10] so they provide a built-in debonding capability that should last for years under ambient conditions. Because of these properties, we concentrated on this class of dyes, specifically F27, to create the ultrathin absorber layer for the debonding experiments.

F27 has two acid groups that can be deprotonated to make it more soluble in hydrophilic solvents and modify its absorption properties.<sup>[11]</sup> We found that the best coating and adhesion properties were obtained when one molar equivalent of NaOH was added to the F27/ethanol solution. Figure 2a shows the SEM Image of a spin-cast F27 film on a smooth PMMA surface, while an optical image is shown in Figure 2b. Both images show homogeneous and smooth films, without visible aggregates or particle formation. The reason that a basic NaOH/F27 solution yields such homogeneous amorphous films is not clear, but we suspect that partial deprotonation provides a good balance between

16 16 30 38, 0, Downloaded from https://onlinelibrary.wiley.com/doi/10.1002/adfm.202410080 by Christopher Bardeen - University Of California, Wiley Online Library on [21/08/2024]. See the Terms and Conditions (thtps://onlinelibrary.wiley.com/terms

and-conditions) on Wiley Online Library for rules of use; OA articles are governed by the applicable Creative Commons!



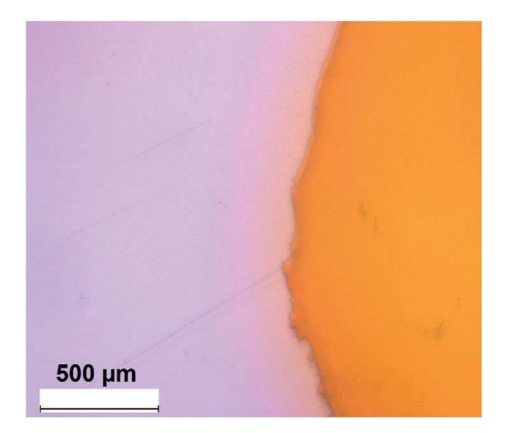
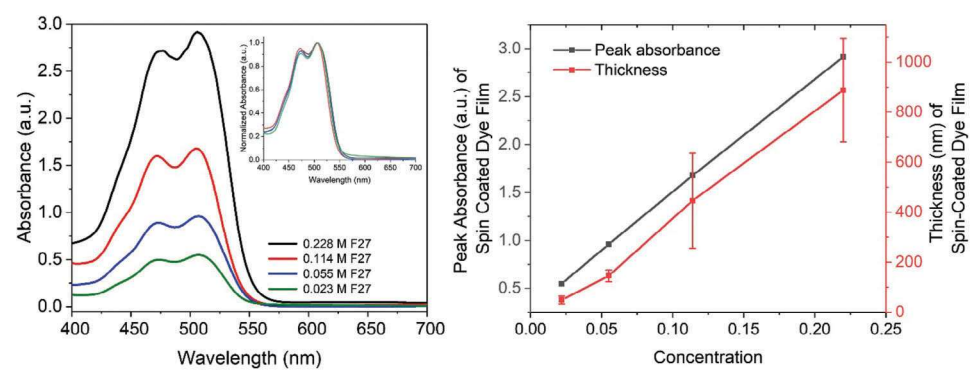


Figure 2. SEM a) and optical b) images of the absorber layer F27 (0.114 M) spin coated onto a smooth PMMA substrate. F27 film occupies the right side of the images.



**Figure 3.** a) UV–vis absorption spectra of F27 layers deposited onto smooth PMMA surfaces. Inset shows normalized spectra, with no change in spectral shape. b) Peak absorbance measured at 515 nm (black) and profilometer thickness measurements (red) of spin-coated films (different precursor concentrations) of F27. The different layers were spin-cast from F27 solutions with different concentrations.

solubility and aggregation during the spin coating process. Partial ionization of the dye may also enhance its interaction with the polar polymer surface, similar to what has been observed for xanthene dyes on polystyrene.  $^{[12]}$  We also tested films spin cast from ethanol solutions containing fully protonated F27 and fully deprotonated disodium F27, but in both cases, the films were much more heterogeneous (Figure S4, Supporting Information).

Variable thickness F27 coatings on the smooth PMMA surfaces were created using precursor solutions with different initial concentrations of F27. The absorption spectra of these films, after subtraction of a scattering background, are shown in Figure **3a.** For all the film spectra, the intensity of the peak at 470 nm was enhanced relative to the solution spectrum, indicating the presence of molecular aggregates as seen both in solution [13] and on surfaces.<sup>[14]</sup> This spectrum was constant for different film thicknesses (Figure 3a, inset), while the peak absorbance increased linearly with precursor concentration (Figure 3b). The film thicknesses were measured using a surface profilometer and also increased linearly with dye concentration, as also shown in Figure 3b. The profilometer traces showed considerable height variation across longer length scales (Figure S5, Supporting Information) and so these thicknesses should be taken as rough estimates for the coatings on the rough PMMA substrates. However, the data clearly show that as the F27 concentration in the

precursor solution increased, the absorbing film thickness increased from  $50\ \text{to}\ 900\ \text{nm}.$ 

In order to make transparent PMMA substrates that could be strongly bonded together by the CA adhesive, their surfaces had to be roughened. To accomplish this in a reproducible manner, we used a lathe treatment to create concentric trenches in the PMMA surface with a peak-to-trough height of 6-7 microns and a radial spacing of  $\approx 100 \, \mu m$  Figure S5 Supporting Information. We checked that spin coating the F27 solutions onto these roughened substrates gave rise to similar absorption behavior, albeit with a larger scattering background (Figure S6, Supporting Information). A ≈100 µm thick layer of CA [15] was used to bond the two roughened PMMA surfaces, one of which had the F27 absorber layer applied. The adhesive strength was then evaluated using an axial butt-joint test using variable applied pressure. The maximum pressure under which the joint survived for 12 h is reported as the adhesive strength. Without the absorbing layer, the adhesive strength was 10 MPa, typical of a "super glue". As the F27 layer thickness increased, the adhesion strength declined but remained in the MPa range, as shown by the plot of the detachment pressure  $P_{detach}$  as a function of thickness in Figure 4. In all cases, the adhesion failed at the interface between the CA and PMMA while the glue layer remained intact.

16162028, 0, Downloaded from https://onlinelibrary.wiley.com/doi/10.1002/adfm.202410080 by Christopher Bardeen - University Of California, Wiley Online Library on [21.08/2024]. See the Terms and Conditions (https://onlinelibrary.wiley.com/terms

and-conditions) on Wiley Online Library for rules of use; OA articles are governed by the applicable Creative Commons

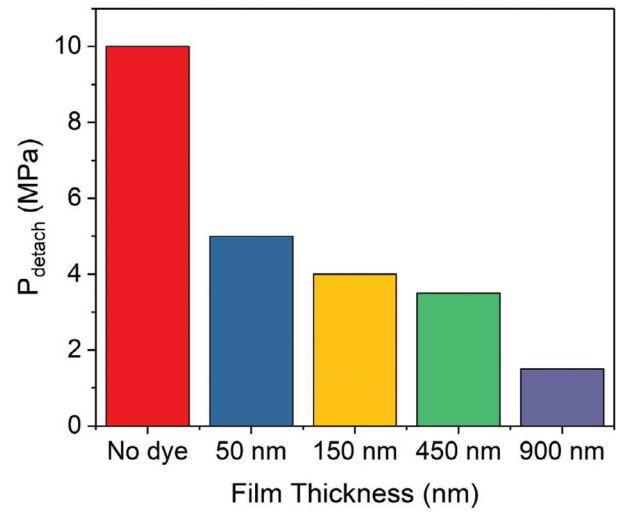


**Figure 4.** The pressure at which detachment occurred ( $P_{detach}$ ) in an axial butt joint adhesion test for different film thicknesses (estimated from profilometer measurements on smooth PMMA films) of F27 on a rough PMMA surface. The precursor solution concentrations that gave rise to the different thicknesses are (from left): 0, 0.023, 0.055, 0.114, and 0.228 M).

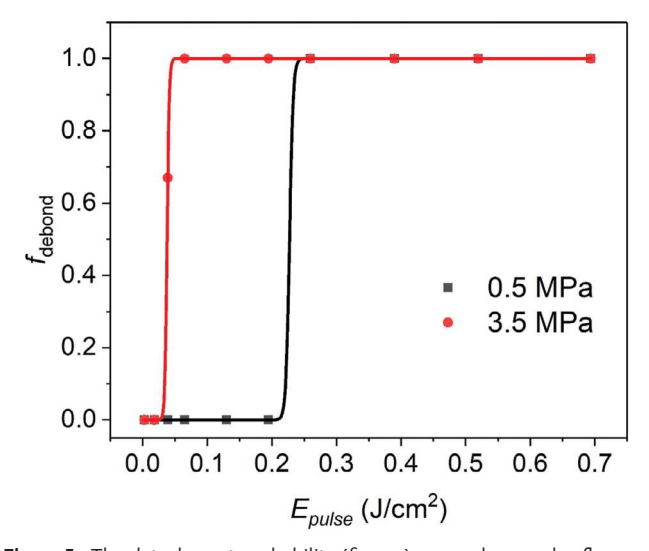


**Figure 5.** The detachment probability ( $f_{\rm debond}$ ) versus laser pulse fluence  $E_{pulse}$  for two different  $P_{appl}$  loading conditions. These measurements were done using an F27 absorber layer created by spin casting a film from a precursor solution with [F27] = 0.114 M (nominal thickness 450 nm) and a 5 ns laser pulse at 532 nm.

We next performed single-shot laser experiments to determine whether the ultrathin absorber films could enable debonding. For the laser debonding experiments, we used a precursor solution with [F27] = 0.11 M, which generated a 450 nm thick film with a peak absorbance of 1.6. This sample could be debonded by a single laser shot at 532 nm with a fluence of 0.7 J cm<sup>-2</sup>, even in the absence of applied pressure. Thinner films provided stronger adhesion but could not be debonded with a single laser shot in the absence of applied pressure. For the 450 nm thick absorber layer, the laser fluence required for debonding decreased as the applied pressure,  $P_{appl}$ , increased. Figure 5 shows two examples

of how the fraction of samples that debond ( $f_{debond}$ ) depends on the laser pulse fluence  $E_{pulse}$  for fixed values of  $P_{appl}$ . Similar to our results with Al, both curves show a clear threshold behavior that can be described using a sigmoidal curve of the form.<sup>[7]</sup>

$$f_{debond} = \frac{1}{1 + \exp\left[\left(-k(E - E_{debond})\right]} \tag{1}$$

where k is the steepness constant and  $E_{debond}$  is the energy fluence threshold for debonding. Fits using Equation (1) are overlaid with the data in **Figure 5**, with  $E_{debond} = 0.038$  J cm $^{-2}$  for  $P_{appl} = 3.5$  MPa, and  $E_{debond} = 0.227$  J cm $^{-2}$  for  $P_{appl} = 0.5$  MPa. For both fits, k was set to 475 cm $^2$  J $^{-1}$ . Varying k by a factor of 2 did not change the quality of the fit or the value of  $E_{debond}$ . As expected, a bond subjected to higher applied pressure can be broken with lower laser fluences. We did not characterize in detail the dependence of  $E_{debond}$  on  $P_{appl}$ , but this limited date set suggests that it is qualitatively similar to that observed for PMMA-CA-Al system. [7]

A comparison of the absorption spectra of a PMMA substrate before and after laser impact (Figure 6a) shows that the F27 absorbance completely vanishes after a single laser pulse. Remarkably, the destruction of the dye layer is not accompanied by largescale changes in the PMMA surface morphology. SEM images of the PMMA surface before coating, after coating, and after laser debonding all show the characteristic ridges imparted by the lathe (Figure 6b–d). The main difference is the presence of small (<50 µm) debris particles scattered across the surface of the debonded sample (Figure 6d). These particles are likely melted PMMA and/or combustion products from the F27. There is no evidence of largescale melting that would smooth the surface ridges. On the other hand, if a continuous wave 532 nm laser was directed onto the adhesive bond, absorption and heating over the course of 20 s eventually caused the bond to fail, but this only occurred after the PMMA surface had completely melted, removing all traces of the original morphology (Figure \$7, Supporting Information).

The creation of reasonably strong adhesive bonds (3.5 MPa), combined with the ability to separate them using a single nanosecond laser pulse, opens up some new capabilities. We constructed a PMMA bolt whose head was attached using CA glue and the absorber layer. This bolt could be inserted through holes drilled in two PMMA beams and a steel nut attached to its threaded end, as shown in Figure 7a. Given the 3.5 MPa adhesive strength of the absorber-CA bond, a bolt with a total mass of 0.5 g and a shank diameter of 5 mm could suspend up to 7.5 kg against gravity. When a single nanosecond laser pulse was directed through the head of the bolt, it caused the head to detach from the shank, which in turn caused the beams to separate, as shown in Figure 7b,c in Video S1 (Supporting Information) in the Supporting Information. The separation occurred within a fraction of a second (faster than the 20 ms resolution of the video camera). This light-powered analog to an exploding bolt also functioned when submerged in water. Although the F27 layer is water soluble in principle, we did not observe any change in the bond strength when submerged in water for 1 h. The rate of dye dissolution from the edges of the absorber layer into the water was apparently negligible on these timescales. When the submerged bolt was exposed to a laser pulse, it was possible to visualize both rapid bubble formation and dye release into

16 16 30 28, 0, Downloaded from https://onlinelibrary.wiley.com/doi/10.1002/adfm.20241 0080 by Christopher Bardeen - University Of California , Wiley Online Library on [21/08/2024]. See the Terms and Conditions (https://onlinelibrary.wiley.com/doi/10.1002/adfm.20241 0080 by Christopher Bardeen - University Of California , Wiley Online Library on [21/08/2024]. See the Terms and Conditions (https://onlinelibrary.wiley.com/doi/10.1002/adfm.20241 0080 by Christopher Bardeen - University Of California , Wiley Online Library on [21/08/2024]. See the Terms and Conditions (https://onlinelibrary.wiley.com/doi/10.1002/adfm.20241 0080 by Christopher Bardeen - University Of California , Wiley Online Library on [21/08/2024]. See the Terms and Conditions (https://onlinelibrary.wiley.com/doi/10.1002/adfm.20241 0080 by Christopher Bardeen - University Of California , Wiley Online Library on [21/08/2024]. See the Terms and Conditions (https://onlinelibrary.wiley.com/doi/10.1002/adfm.20241 0080 by Christopher Bardeen - University Of California , Wiley Online Library on [21/08/2024]. See the Terms and Conditions (https://onlinelibrary.wiley.com/doi/10.1002/adfm.20241 0080 by Christopher Bardeen - University Of California , Wiley Online Library on [21/08/2024]. See the Terms and Conditions (https://onlinelibrary.wiley.com/doi/10.1002/adfm.20241 0080 by Christopher Bardeen - University Of California , Wiley Online Library on [21/08/2024].

and-conditions) on Wiley Online Library for rules of use; OA articles are governed by the applicable Creative Commons License

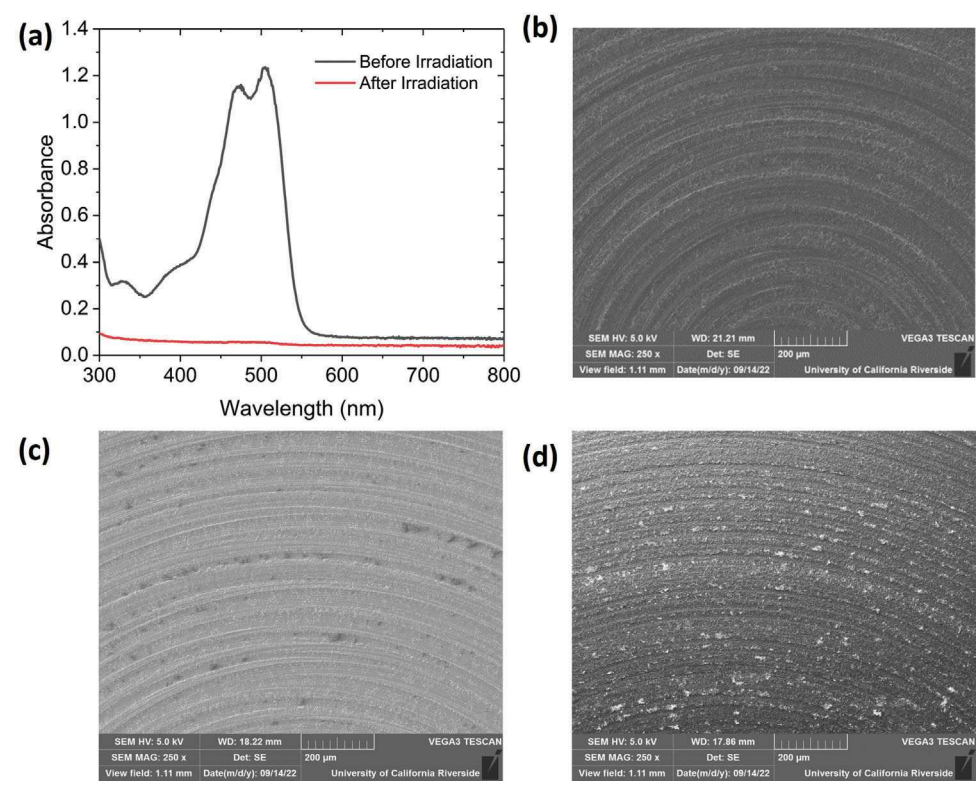


**Figure 6.** a) Absorbance of a 400 nm thick spin-coated F27 layer on a rough PMMA substrate before (black) and after (red) irradiation by a single laser pulse with  $E_{pulse} = 0.7 \, \text{J cm}^{-2}$ . b) Roughened PMMA surface before spin coating. c) Roughened PMMA surface after spin coating with F-27. The contrast has changed due to the different conductivity of the dye layer. d) Roughened PMMA surface with dye layer after irradiation with a single laser pulse at 532 nm with  $E_{pulse} = 0.7 \, \text{J cm}^{-2}$ .

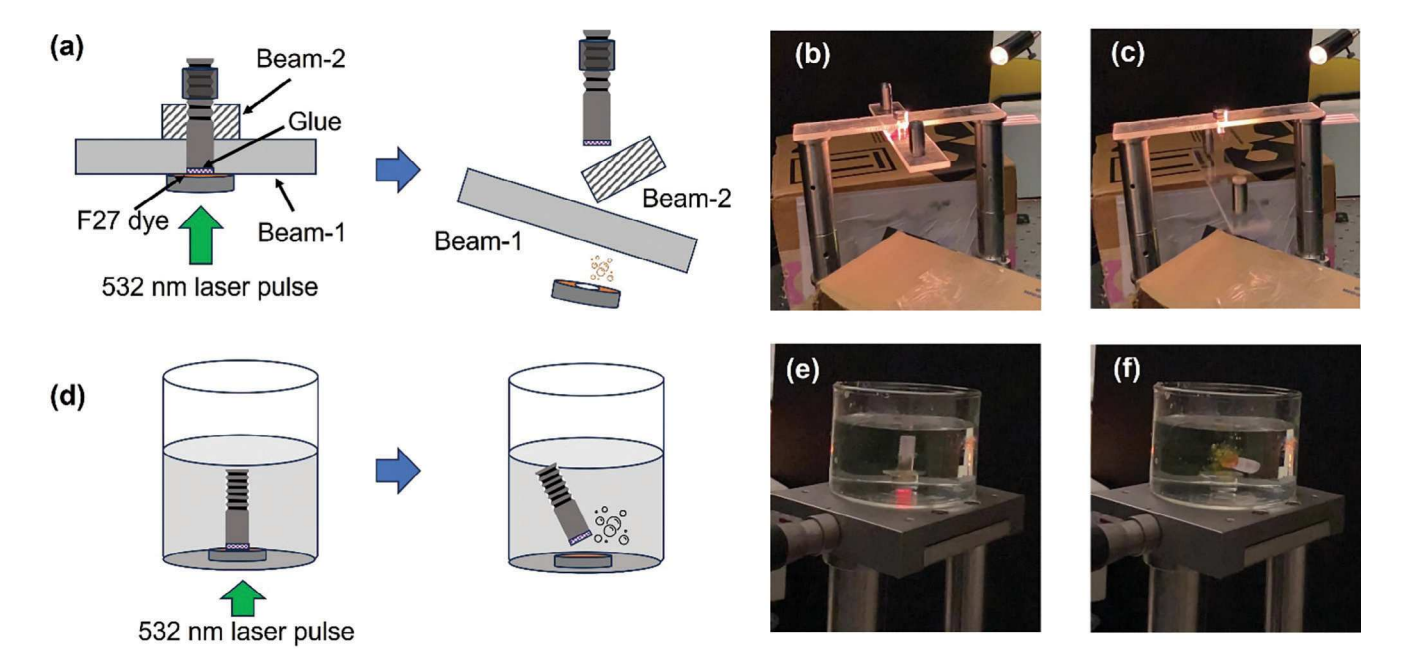


**Figure 7.** a) Schematic diagram of PMMA bolt holding two plastic beams separating with a single shot laser pulse. Photographs of the PMMA beam assembly before b) and after c) a single laser pulse (532 nm, 0.7 J cm $^{-2}$ ) separates the bolt, causing the bottom beam to fall. d) Schematic diagram of PMMA bolt separation underwater. Photographs of the plastic bolt before e) and after f) a single laser pulse (532 nm, 0.7 J cm $^{-2}$ ) separates the bolt, generating bubbles and dissolved dye.

www.afm-journal.de

1616303.0, Downloaded from https://onlinelbtrary.wiley.com/doi/10.002/adfm:002/10.002/adfm:002410800 by Christopher Bardeen - University Of California, Wiley Online Library on [21/082024]. See the Terms and Conditions (https://onlinelbrary.wiley.com/terms-and-conditions) on Wiley Online Library for rules of use; OA articles are governed by the applicable Creative Commons License

the surrounding water after the separation event, as shown in Figure 7e,f, and in Video S2 (Supporting Information).

The single-shot laser debonding relies on the ability of the F27 layer to transform the incident laser light into heat on the nanosecond timescale. Although individual F27 molecules isolated in solution have high fluorescence quantum yields of 0.96, [16] fluorescein aggregates have very low fluorescence quantum yields, [13b,17] and nonradiative relaxation that turns the photon energy into heat becomes dominant. The amount of heat deposited during the 5 nanosecond pulse can be roughly estimated by assuming every F27 molecule absorbs one photon during the pulse. If we assume a dye density of 1.5 g cm<sup>-3 [18]</sup> and a molecular weight of 401.2 g mol<sup>-1</sup>, we can estimate that an energy density of ≈1000 J cm<sup>-3</sup> is deposited during the pulse. Given PMMA's low thermal diffusivity of  $\approx 10^{-3}$  cm<sup>2</sup> s<sup>-1</sup>, [19] this heat will only diffuse over 50 nm during the pulse, effectively localizing it at the absorbing interface. Taking the heat capacity of the absorber layer to be similar to that of PMMA (1.5 J  $g^{-1}$   $K^{-1}$ ), [20] this energy density will lead to a temperature jump of ≈650 K, which is sufficient to pyrolyze organic molecules.[21] Thus we expect this heating to not only melt the glue and substrate, but also to produce a high-temperature gas expansion.

Several experimental observations are consistent with rapid, localized thermal decomposition of the organic dye layer. The lack of extensive damage or deformation of the PMMA surface trenches suggests that substrate melting does not play a decisive role in the debonding. The observation of gas evolution in the underwater experiments, in the form of bubbles, is consistent with the decomposition of F27 into gas phase molecules. Previous work has shown that pyrolysis of fluorescein produces gaseous CO, O<sub>2</sub>, and small alkenes, [22] while photochemical decomposition also yields CO and CHOOH. [23] Direct characterization of the volatile decomposition products would provide insight into the chemical mechanisms of debonding and will be the subject of future work. Rapid gas expansion is consistent with the fact that the laser impact could actually propel the body of the screw upward after debonding. The amount of force generated by superheated gas produced by chemical decomposition and vaporization can be significant, with up to several percent of the incident laser energy being converted to kinetic energy of the absorbing piece. [24] Given these observations, we hypothesize that the rapid thermal decomposition of the absorber layer leads to two outcomes. First, physical contact between the CA and PMMA layers is lost as the intermediate absorber layer decomposes. Second, the expanding gas products of this decomposition provide an extra force that helps rupture any remaining bonds. Determining the relative importance of these two effects, along with the chemical pathways for gas generation, will be a subject for future work.

Although it has the advantages of being rapid, nondestructive, and compatible with strong adhesives, we should also note that nanosecond laser debonding has some limitations. First, the light must be able to directly access the adhesive interface, which requires that at least one substrate be transparent to the laser wavelength. Second, it is irreversible in the sense that the adhesion cannot be recovered without applying a new layer of glue. Third, the insertion of an absorbing layer weakens the bond by ≈50% by decreasing the interfacial strength. Whether this is acceptable will depend on the application, but it is clear that adding the debonding capability comes at a cost to the initial adhesive strength.

## 3. Conclusion

In this paper, we have shown that the nanosecond laser debonding method can be extended to transparent substrates. The deposition of an ultrathin (<1 µm) absorbing layer before gluing can maintain reasonably strong adhesion while building in a way to induce rapid bond failure through the application of a pulsed light source. In this work, the absorbing layer is composed of F27 dye aggregates which combine high absorbance with efficient photothermal degradation. For example, a 450 nm thick F27 layer retained an adhesive strength of 3.5 MPa while enabling singleshot debonding with a 532 nm nanosecond laser pulse with fluences on the order of 0.7 I cm<sup>-2</sup> or less. Remarkably, this debonding did not melt or damage the PMMA surface to a significant extent. This system enabled us to design an optical analog of the exploding bolt, where a single light pulse caused rapid separation of the bolt accompanied by structure dismantling. Although we have focused on the PMMA-CA-PMMA system to demonstrate the general concept, it should be applicable to a wide range of adhesives and substrates. The challenge will be to find a combination of molecular absorber and layer thickness that is compatible with the transparent substrate while preserving an acceptable level of adhesive strength. A submicron-thick conformal absorber coating is all that is needed to transform an irreversible bond into a reversible bond, without the need to develop completely new adhesives. This capability could be built into glued structures so that they can easily be disassembled by a laser for recycling or

### 4. Experimental Section

Sample Preparation: Cyanoacrylate (CA) adhesive (3 M Scotch-Weld Instant Adhesive CA8) was used to glue two transparent poly(methyl methacrylate) (PMMA) substrates purchased from McMaster-Carr (part number 8531K23). 2',7'-dichloro-3',6'-dihydroxyspiro[2-benzofuran-3,9'xanthene]-1-one, commonly known as Fluorescein 27 (F27), was purchased from Lambda Physik (stock number LC 5530). Ethanol (200 Proof) was purchased from Fisher Scientific-USA (Catalogue number BP2818). The disodium salt of F27 was purchased from Tokyo Chemical Industry-USA (stock number D0424).

To prepare samples for adhesion testing, a PMMA disk, roughened by a lathe treatment to improve adhesion, was wiped with a solution of 30% isopropyl alcohol in water. A basic solution of F27 was prepared by dissolving F27 in ethanol and adding a volume of aqueous NaOH solution (0.6 M) to achieve a 1:1 molar ratio. A typical sample involved mixing 3.6 mL of an ethanol solution with 0.11 M F27 with 0.61 mL of 0.6 M NaOH in water. The F27 dye solution was spin-coated onto the PMMA disk with a spin coater (WS-400B-6NPP/Lite, 60 µL, 1000 RPM, 30 s) and left to dry for 15 min. The CA adhesive was then drop-cast on the spin coated surface, and a threaded PMMA cylinder was pressed onto it. The sample was left to cure in air for at least 24 h. Additional preparation details are provided in Figure S1 (Supporting Information).

Characterization: Scanning electron microscope (SEM) images were acquired using a Nova NanoSEM (NNS450 SEM). A Leica DM2700 M microscope was used for optical imaging. For UV-vis absorption measurements of solid dye films, the dye solution was spin-coated onto the PMMA substrates. An Agilent Cary 60 UV-vis spectrophotometer was used to take the absorption spectra. Surface profile measurements for spin-coated dye



www.advancedsciencenews.com



www.afm-journal.de

16163028, 0, Downloaded from https://onlinelibrary.wiley.com/doi/10.1002/adfm.202410080 by Christopher Bardeen - University Of California, Wiley Online Library on [21/08/2024]. See the Terms

and Conditions (https://onlinelibrary.

of use; OA articles are governed by the applicable Creative Commons

layer thickness for different concentrations were acquired with a Stylus Profilometer (Veeco Dektak-8).

Pulsed Laser Debonding: A custom-built experimental setup was used to measure the adhesive strength of the glued samples and characterize the laser-based debonding, as detailed in the previous work. [7] Briefly, a pulley system was designed and integrated with a nanosecond (5 ns) pulsed laser (Amplitude Surelite II-10) with a single shot capability. The wavelength was changed from the fundamental at 1064 nm (maximum pulse energy  $\approx$ 685 mJ) to the second harmonic at 532 nm (maximum pulse energy  $\approx$ 285 mJ) by frequency doubling. The laser fluence was attenuated by delaying the Q-Switch to reduce the power. The pulse energy was measured with a power meter (Newport 843-R). A number of samples (3–5) were tested at each pulse energy to determine  $f_{debond}$ . Multiple samples were also used for different adhesion pressure tests, with the average value being reported. The variation between samples was on the order of 10%, so a full statistical analysis was not performed.

# **Supporting Information**

Supporting Information is available from the Wiley Online Library or from the author.

# Acknowledgements

This work was supported by the National Science Foundation DMR-1810514.

## **Conflict of Interest**

The authors declare no conflict of interest.

## **Data Availability Statement**

The data that support the findings of this study are available from the corresponding author upon reasonable request.

#### **Keywords**

adhesion, cyanoacrylate, debond, dye, nanosecond, photothermal

Received: June 10, 2024 Revised: July 22, 2024 Published online:

[1] a) A. C. Marques, A. Mocanu, N. Z. Tomić, S. Balos, E. Stammen, A. Lundevall, S. T. Abrahami, R. Günther, J. M. M. d. Kok, S. T. d. Freitas,

- Materials. 2020, 13, 5590; b) S. Maggiore, M. D. Banea, P. Stagnaro, G. Luciano, Polymers. 2021, 13, 3961.
- [2] a) C. Bandl, W. Kern, S. Schlögl, Int. J. Adhesion Adhes. 2020, 99, 102585; b) Z. Liu, F. Yan, Adv. Sci. 2022, 9, 2200264.
- [3] K. R. Mulcahy, A. F. R. Kilpatrick, G. D. J. Harper, A. Walton, A. P. Abbott, Green Chem. 2022, 24, 36.
- [4] J. Lee, J.-H. Han, Y. Lee, H. Lee, Aerosp. Sci. Technol. 2014, 39, 153.
- a) A. Hutchinson, Y. Liu, Y. Lu, J. Adhesion. 2017, 93, 737; b) M. D. Banea, L. F. M. d. Silva, R. J. C. Carbas, S. d. Barros, J. Adhesion. 2017, 93, 756; c) H. Caglar, I. Sridhar, M. Sharma, K. S. Chian, J. Adhesion. 2022, 99, 1626.
- [6] a) C. Heinzmann, S. Coulibaly, A. Roulin, G. L. Fiore, C. Weder, ACS Appl. Mater. Interfaces. 2014, 6, 4713; b) R. H. Zha, G. Vantomme, J. A. Berrocal, R. Gosens, B. Waal, S. Meskers, E. W. Meijer, Adv. Funct. Mater. 2018, 28, 1703952; c) T. Yamamoto, Y. Norikane, H. Akiyama, Polym. J. 2018, 50, 551; d) D. K. Hohl, C. Weder, Adv. Opt. Mater. 2019, 7, 1900230; e) Y. Gao, K. Wu, Z. Suo, Adv. Mater. 2019, 31, 1806948; f) W.-C. Xu, S. Sun, S. Wu, Angew. Chem., Int. Ed. 2019, 58, 9712; g) J. Yang, R. Bai, B. Chen, Z. Suo, Adv. Funct. Mater. 2020, 30, 1901693; h) T. J. Gately, W. Li, S. H. Mostafavi, C. J. Bardeen, Macromolecules. 2021, 54, 9319; i) M. Aizawa, H. Akiyama, T. Yamamoto, Y. Matsuzawa, Langmuir. 2023, 39, 2771.
- [7] T. B. Anwar, T. N. Lewis, A. J. Berges, T. J. Gately, C. J. Bardeen, J. Adhesion. 2024, 100, 186.
- [8] S. Kavda, S. Golfomitsou, E. Richardson, Heritage Sci. 2023, 11, 63.
- [9] M. C. Adams, J. Davis, Geothermics. 1991, 20, 53.
- [10] C. Eggeling, J. Widengren, R. Rigler, C. A. M. Seidel, *Anal. Chem.* 1998, 70, 2651.
- [11] R. Sjöback, J. Nygren, M. Kubista, Spect. Chim. Acta A. 1995, 51, L7.
- [12] M. Mullen, N. Fontaine, W. B. Euler, J. Fluoresc. 2020, 30, 811.
- [13] a) J. E. Selwyn, J. I. Steinfeld, J. Phys. Chem. 1972, 76, 762; b) O. Valdes-Aguilera, D. C. Neckers, Acc. Chem. Res. 1989, 22, 171.
- [14] E. Novoa-Ortega, M. Dubnicka, W. B. Euler, J. Phys. Chem. C. 2020, 124, 16058.
- [15] D. M. Gleich, M. J. L. V. Tooren, A. Beukers, J. Adhesion Sci. Tech. 2001, 15, 1091
- [16] X.-F. Zhang, J. Zhang, L. Liu, J. Fluoresc. 2014, 24, 819.
- [17] J. Mei, Y. Hong, J. W. Y. Lam, A. Qin, Y. Tang, B. Z. Tang, Adv. Mater. 2014, 26, 5429.
- [18] S. V. Hering, S. K. Frledlander, J. J. Collins, L. W. Richards, Env. Sci. Technol. 1979, 13, 184.
- [19] M. Rohde, F. Hemberger, T. Bauer, J. Blumm, T. Fend, T. Hausler, U. Hammbrschmidt, W. Hohenauer, K. Jaenicke-Rossler, E. Kaschnitz, E. Pfaff, G. Pintsuk, High Temp. High Press. 2013, 42, 469.
- [20] https://webbook.nist.gov/, NIST Chemistry WebBook, SRD 69, (accessed: April, 2024).
- [21] a) I. Safarik, O. P. Strausz, Res. Chem. Intermed. 1996, 22, 275; b) I. Safarik, O. P. Strausz, Res. Chem. Intermed. 1997, 23, 63.
- [22] M. Arshad, K. Masud, A. Saeed, A. H. Qureshi, G. Shabir, J. Therm. Anal. Calorim. 2018, 131, 1385.
- [23] M. Martínek, L. Ludvíková, M. Šranková, R. Navrátil, L. Muchová, J. Huzlík, L. Vítek, P. Klán, P. Šebej, Org. Biomolec. Chem. 2023, 21, 93.
- [24] T. N. Lewis, C. J. Bardeen, Appl. Phys. A. 2023, 129, 189.